ResearchGate

See discussions, stats, and author profiles for this publication at: https://www.researchgate.net/publication/264220040

Wavelength-Emission Tuning of ZnO Nanowire-Based Light-Emitting Diodes by Cu Doping: Experimental and Computational Insights

ARTICLE *in* ADVANCED FUNCTIONAL MATERIALS · SEPTEMBER 2011

Impact Factor: 11.81 · DOI: 10.1002/adfm.201100258

CITATIONS
77

READS
113

5 AUTHORS, INCLUDING:

Lupan Oleg
University of Central Florida
136 PUBLICATIONS **3,550** CITATIONS
SEE PROFILE

Thierry Pauporté
Chimie ParisTech
163 PUBLICATIONS **4,711** CITATIONS
SEE PROFILE

Tangui Le Bahers
Claude Bernard University Lyon 1
33 PUBLICATIONS **854** CITATIONS
SEE PROFILE

Bruno Viana
École nationale supérieure de chimie de Paris
386 PUBLICATIONS **5,539** CITATIONS
SEE PROFILE

Available from: Thierry Pauporté
Retrieved on: 24 January 2016

Wavelength-Emission Tuning of ZnO Nanowire-Based Light-Emitting Diodes by Cu Doping: Experimental and Computational Insights

Oleg Lupan, Thierry Pauporté, Tangui Le Bahers, Bruno Viana, and Ilaria Ciofini*

The band-gap engineering of doped ZnO nanowires is of the utmost importance for tunable light-emitting-diode (LED) applications. A combined experimental and density-functional theory (DFT) study of ZnO doping by copper (Zn^{2+} substitution by Cu^{2+}) is presented. ZnO:Cu nanowires are epitaxially grown on magnesium-doped p-GaN by electrochemical deposition. The heterojunction is integrated into a LED structure. Efficient charge injection and radiative recombination in the Cu-doped ZnO nanowires are demonstrated. In the devices, the nanowires act as the light emitters. At room temperature, Cu-doped ZnO LEDs exhibit low-threshold emission voltage and electroluminescence emission shifted from the ultraviolet to violet–blue spectral region compared to pure ZnO LEDs. The emission wavelength can be tuned by changing the copper content in the ZnO nanoemitters. The shift is explained by DFT calculations with the appearance of copper d states in the ZnO band-gap and subsequent gap reduction upon doping. The presented data demonstrate the possibility to tune the band-gap of ZnO nanowire emitters by copper doping for nano-LEDs.

1. Introduction

The emerging fields of nanotechnology and nanoelectronics have attracted intense attention, notably with promising new low-dimensional optoelectronic devices with multifunctionality capabilities. Zinc oxide (ZnO) is a semiconductor with a wide and direct band-gap (3.37 eV at room temperature).[1] By doping zinc oxide with selected elements, it is possible to achieve versatile and desirable optical, electrical, or magnetic properties which are very important for device applications.[2]

Recently, ZnO nanoarchitectures, such as nanowires (NWs) and nanorods (NRs) have been a focus of research interest for transparent conducting contacts, photodetectors, nanolasers, low-dimensional light emitters, light-emitting-diode (LED) screens, and solid-state lighting.[3–5] ZnO has a strong exciton binding energy (60 meV compared to 25 meV for GaN)[3,7] which should favor the development of ZnO-LEDs that are much brighter than the corresponding GaN light emitters.[8] However, ZnO is intrinsically n-type due to native defects and the fabrication of reproducible and stable p-type zinc oxide semiconductors is difficult, which makes the fabrication of nano-ZnO-based homojunction devices problematic. For such devices, a useful heterojunction is required that can be fabricated by using another p-type material with lattice constants well-matched to that of ZnO. This matching is important because lattice mismatch could introduce dislocations resulting in interface states between the two materials and reduced efficiency of the LEDs.

ZnO and GaN have the same wurtzite crystal structure with similar lattice parameters and a small in-plane lattice mismatch (ca. 1.9% for the *a* parameter).[6] ZnO NW/p-GaN films are promising heterostructures for nano-LEDs because nanowires can act as direct waveguides and favor light extraction without the use of lenses and reflectors.[3] Also, the emitted light from ZnO NWs/p-GaN film heterojunctions is confined within the nanowire and will be optically transmitted accordingly to the effective medium theory.

Reliable ultraviolet (UV) emission from ZnO-based device structures has been already demonstrated at both low and room temperatures.[3,4,10,11] However, for practical applications, it is important to develop an efficient technique for tuning the emission wavelength by engineering the band-gap of the nanomaterial. The literature is extensive about the band-gap tuning of ZnO films by addition of dopants.[9–15] Doping is also important to create quantum wells which facilitate radiative recombination by carrier confinement.[13] However, several issues have to be clarified, such as the possibility of doping NWs through a cost-effective and efficient electrochemical process, to tune their chemical and physical properties by incorporation of dopant into the lattice of ZnO. Copper is a prominent

Dr. O. Lupan,[+] Dr. T. Pauporté, T. Le Bahers, Dr. I. Ciofini
Chimie ParisTech
Laboratoire d'Electrochimie
Chimie aux Interfaces et Modélisation pour l'Energie (LECIME)
UMR 7575 CNRS, 11 rue P. et M. Curie, 75231 Paris, cedex 05, France
E-mail: thierry-pauporte@chimie-paristech.fr
Dr. B. Viana
Chimie ParisTech
Laboratoire de Chimie de la Matière Condensée de Paris
UMR 7574, 11 rue P. et M. Curie, 75231 Paris cedex 05, France
[+] Present address: Department of Microelectronics and Semiconductor Devices, Technical University of Moldova, 168 Stefan cel Mare Blvd., Chisinau, MD-2004, Republic of Moldova

DOI: 10.1002/adfm.201100258

© 2011 WILEY-VCH Verlag GmbH & Co. KGaA, Weinheim

luminescence activator in II–VI semiconductors.[14,15] Investigation of the effects of doping with copper on the structural and optical properties of ZnO nanowires grown by electrochemistry could be useful for synthesis of conductive $Zn_{1-x}Cu_xO$ nanostructures, which can lead to the fabrication of spin LEDs and switchable spin-laser diodes. The high ionization energy of copper and the low formation energy of substitutional group IB elements indicate that high concentrations of Cu could be incorporated into ZnO, which could be used for band-gap engineering.[16,17] According to previous theoretical reports[17–19] new bands can form inside the ZnO band-gap by means of Cu doping, which narrow the band-gap significantly. Experimentally, it was observed that Cu substituted at the Zn site exhibited defect states in the ZnO band-gap located at –0.17 eV below the bottom of the conduction band[18] and at +0.45 eV above the valence band.[19] In recent reports, a greenish-blue emission peak was observed for a Cu-doped ZnO film based LED device fabricated by using plasma-assisted molecular beam epitaxy[20] and by the filtered cathodic vacuum technique.[21] The large p–d coupling between the group-IB d state and the oxygen p state also suggests that the effective mass of the defect band will be small, and will favor transport properties.[17,22]

Various techniques such as the vapor–liquid–solid (VLS) process, chemical-vapor deposition, metal-organic chemical-vapor deposition (MOCVD), and thermal diffusion have been employed to synthesize ZnO:Cu NWs/NRs.[23–28] However, to the best of our knowledge, no report has appeared on ZnO:Cu NW based LED structures with tuned electroluminescence emission at room temperature. We have recently developed electrochemical deposition (ECD) as a low–temperature solution-growth method for fabricating high quality ZnO-NW-based heterojunctions[3,4,29] and we have fabricated low voltage UV-LEDs with strong UV emission at room temperature.[3,4] To explore the possible band tuning of ZnO NWs we study here Cu doping during the electrochemical growth of ZnO NWs on p-GaN substrates for LED applications.

Herein, nanomaterial properties of electrodeposited ZnO:Cu NWs on p-GaN and its device integration are presented for the first time. LED structures based on (n-ZnO:Cu NW)/(p-Mg:GaN film) heterojunctions are experimentally studied. To further support the analysis of the experimental data, a computational DFT protocol is applied, which further confirms the possibility to tune the band-gap of ZnO NWs by Cu doping. Taken together, these results demonstrate the possibility to engineer the band-gap of ZnO NWs by copper doping and thus tuning of the emission wavelength of LED structures. The method developed here is novel, cost-effective, well-controlled, low-temperature, and takes place in nonaggressive environments; it could be suitable for any type of doping in ZnO NWs and is of great importance for further investigations/applications.

2. Results and Discussion

ZnO nanowires were grown on (0001)-oriented Mg-doped p-GaN single crystalline films and Cu doping was achieved by adding $CuCl_2$ to the deposition solution. Cu was detected in the wires by using energy-dispersive X-ray spectroscopy (EDX) and the content was found to increase with the Cu(II) concentration in the bath. The top-view scanning electron microscopy (SEM) image of Cu-doped ZnO NWs grown on p-GaN substrates at 90 °C (**Figure 1**a) is representative of epitaxial ZnO wires[3] with hexagonal facets oriented in the same direction. The inset is a cross-sectional view of the ZnO:Cu/GaN heterostructure, which shows that the nanowires grow perpendicular to the substrate as expected for an epitaxial growth of ZnO:Cu along the *c* axis.[4] The high structural/optical quality of the deposited wires was characterized by various techniques. Figure 1b displays X-ray diffraction (XRD) patterns of pure and Cu-doped ZnO NWs. These patterns contain ZnO peaks for pure and Cu-doped ZnO NWs, along with reflections from the GaN substrate. The pattern matches the lattice spacing of wurtzite ZnO (space group: $P6_3mc$(186); a = 0.3249 nm, c = 0.5206 nm). The data are in agreement with the Joint Committee on Powder Diffraction Standards (JCPDS) card for ZnO (JCPDS 036-1451). The XRD shows only (0002*l*)ZnO planes due to a growth orientation of the NWs on p-GaN with the *c* axis perpendicular to the substrate. To study the effect of Cu doping on the crystallinity of the ZnO nanowires and control the Cu insertion into the ZnO lattice, the position of the ZnO(0002) diffraction peak was monitored. There was a small shift of ca. 0.04° to a higher 2θ angle value of the ZnO(0002) XRD diffraction peaks for low Cu doping, compared to that of pure ZnO (Figure 1b inset). The lattice constant *c* was estimated at 5.2055 Å for pure ZnO NWs and 5.1981 Å for ZnO:Cu. A slight lattice deformation of nanocrystals can be suggested for ZnO:Cu. This result indicates that Cu atoms are introduced into the ZnO wurtzite lattice and that a slight lattice deformation of nanocrystals may occur for ZnO:Cu, considering that the ionic radii of Cu^{2+} and Zn^{2+} are 0.054 nm and 0.074 nm, respectively.[30] This deformation should lead to shorter Cu_{Zn}–O bonds and smaller $[Cu_{Zn}O_4]$ units in the Cu-doped ZnO material.[31] The full width at half maximum (FWHM) of the (002) peak (Figure 1a) increased for Cu-doped samples from 0.06° (pure ZnO) to 0.11° (ZnO:Cu), which suggests that Cu incorporation into the lattice increases disorder. Such changes in crystallinity might be the result of changes in the atomic environment due to extrinsic doping of ZnO samples. Due to the low formation energy of Cu in ZnO under O-rich conditions, high concentration of dopants can be easily achieved with copper.[17] We found similar results for various concentrations of $CuCl_2$ in the bath (3–15 μM $CuCl_2$), which suggest Cu incorporation into the lattice with a concentration up to 3 at.% Cu (data not shown).

To support our experimental observations we performed a computational study based on density functional theory (DFT) of Cu-doped ZnO. Figure 1c presents the supercell of the ZnO doped with 1.8 at.% copper. Results obtained for two other Cu concentrations can be found in **Table 1**. Cell parameters of pure ZnO are computed to be 3.333 Å and 5.172 Å for *a* and *c*, respectively. In the presence of copper these parameters are only slightly reduced with *a* and *c* equal to 3.329 Å and 5.166 Å. This decrease is consistent with the experimental observations discussed above, which thus confirms the accuracy of the adopted computational protocol. In pure ZnO, Zn atoms have a tetrahedral coordination with a computed Zn–O distance of 2.004 Å. In Cu-doped ZnO the Cu_{Zn} environment is no longer a regular tetrahedron, with a shorter Cu_{Zn}–O (1.875 Å) distance

© 2011 WILEY-VCH Verlag GmbH & Co. KGaA, Weinheim

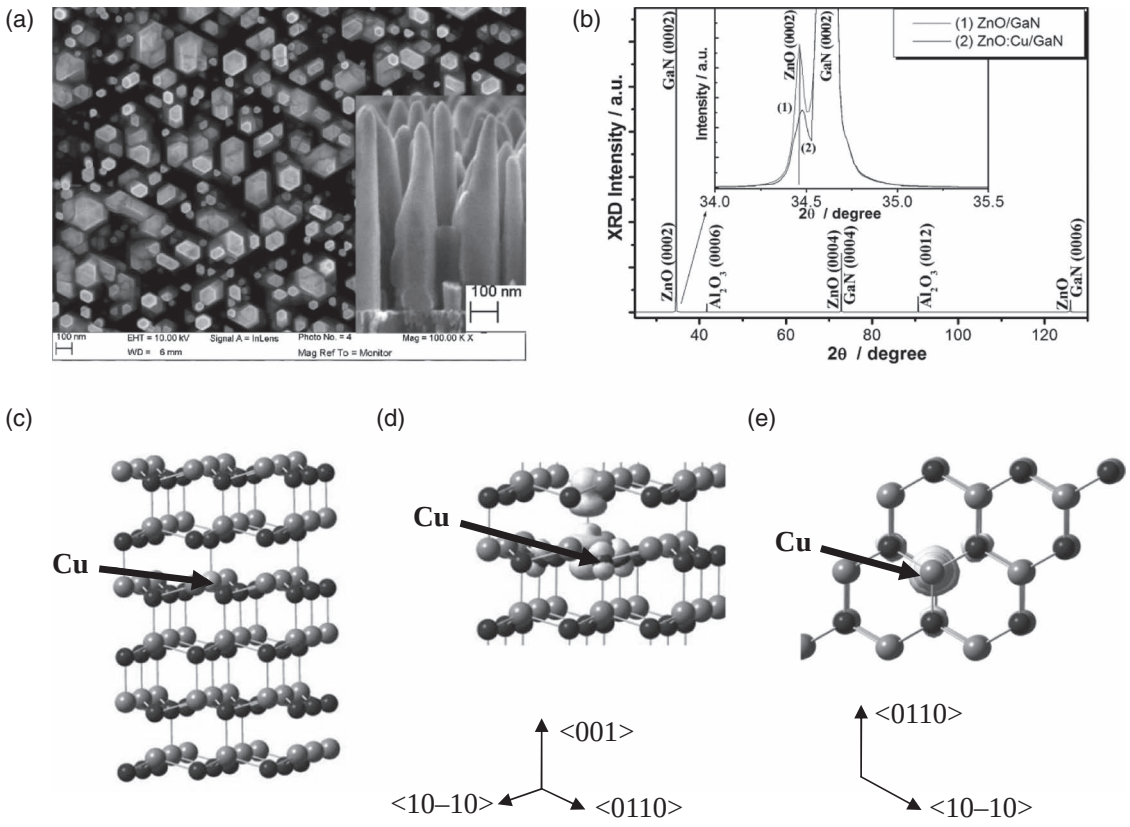

Figure 1. a) SEM image (top view) of epitaxial ZnO nanowires electrochemically grown on p-GaN substrate at 90 °C and the cross-sectional view as an inset. b) XRD pattern of the ZnO:Cu-NW/p-GaN/Al_2O_3 (0001) structure. Inset: Enlarged view for the comparison of ZnO/GaN and ZnO:Cu/GaN (0002) peaks. c–e) Computed optimized structure of Cu-doped ZnO (1.8 at.%). d,e) Different views of the computed spin density of the copper-doped ZnO system. The color scheme is black, gray, and pale gray for oxygen, zinc, and copper atoms, respectively, and white for the excess of α spins.

along the *c* axis and 2 + 1 Cu–O distances at 1.965 Å and 1.971 Å. The same type of coordination was also computed by Ye et al.[32] This deformation is a consequence of a Jahn–Teller distortion, effective for tetrahedral d^9 metal ions, such as Cu^{2+}. This structural finding supports the hypothesis that the copper inserted into the ZnO lattice is a Cu^{2+} ion. Overall, the presence of Cu atoms only slightly modifies the ZnO structure, which is in good agreement with the ability of ZnO to accept a rather high quantity of Cu atoms as dopant.

Table 1. Computed effects of copper doping on the wurtzite lattice parameters [*a*, *b*, *c*, α (angle between the *b* and *c* axis), β (angle between the *a* and *c* axis), and γ (angle between the *a* and *b* axis)] and copper to oxygen distances. Electronic gap of the system computed for α and β spins, respectively ($E_{gap,\alpha}$ $E_{gap,\beta}$).

ZnO	ZnO:Cu	ZnO:Cu	ZnO:Cu	
at.% Cu	0.00	0.78	1.85	6.25
a[Å]	3.333	3.329	3.329	3.327
b[Å]	3.333	3.332	3.332	3.302
c[Å]	5.172	5.176	5.166	5.171
α[°]	90.00	90.00	90.00	90.00
β[°]	90.00	90.00	89.99	90.16
γ[°]	120.00	120.03	120.03	119.75
Cu-O^1 [Å]	2.004	1.970	1.971	1.978
Cu-O^2 [Å]	2.004	1.967	1.965	1.909
Cu-O^3 [Å]	2.004	1.967	1.965	1.909
Cu-O^4 [Å]	2.004	1.875	1.875	2.025
$E_{gap,\alpha}$	3.93	3.90	3.85	3.93
$E_{gap,\beta}$	3.93	3.76	3.65	3.47

Dopant influence on ZnO NWs was also investigated by Raman spectroscopy. **Figure 2**a shows Raman peaks typical of the wurtzite structure for pure and Cu-doped ZnO NWs on p-GaN. From the inset in Figure 2a, one can observe the influence of Cu doping on the E_2(high) mode of ZnO. The intensity of this peak decreases for doped ZnO NWs and shows a strong signal shift from 439 to ca. 437 cm^{-1} with respect to pure ZnO NWs. A similar shift was also found for ZnO:Cu grown by other techniques.[23,33–35] The frequency shift was explained by alloy potential fluctuation (APF) using the spatial correlation model by Samanta et al.[36] Also, it is clearly observed that for ZnO:Cu the Raman line E_2(high) mode becomes increasingly broad and weak, which means that the structural quality of the wurtzite crystalline structure of ZnO NWs is reduced by higher Cu doping.[34] These data are in agreement with the XRD patterns of ZnO NWs described above.

The optical quality and the wavelength-emission changes with copper doping were investigated by means of photoluminescence (PL) spectroscopy. In Figure 2b, the p-GaN PL spectrum is characterized by a strong emission with a single peak

© 2011 WILEY-VCH Verlag GmbH & Co. KGaA, Weinheim

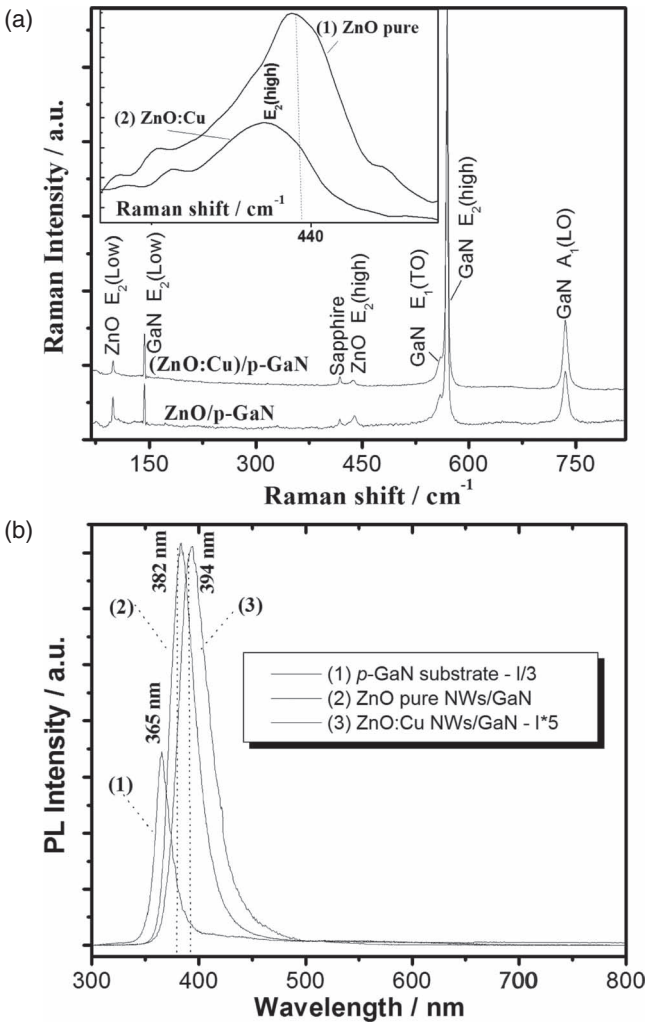

Figure 2. a) Raman spectra of epitaxial ZnO and ZnO:Cu-NWs electrodeposited on p-GaN thin film. Inset: Influence of Cu doping on the E_2(high) mode of ZnO nanowires. b) Photoluminescence spectra of the epitaxial ZnO-NWs/p-GaN and ZnO:Cu-NWs/p-GaN heterojunctions and of p-GaN substrate. $T = 300$ K.

located at 365 nm and an FWHM of 16 nm. No blue emission due to a transition between the conduction band and deep Mg-dopant levels was observed for the substrate in our experiments. For ZnO/p-GaN structure, only a ZnO near-band-edge emission centered at 382 nm with an FWHM of 30 nm was detected. The absence of visible emission is the signature of a very high quality material with a low defect density.[37] The PL emission from ZnO:Cu/p-GaN structure had the same shape as pure ZnO/p-GaN (curve 2, Figure 2b). ZnO:Cu was of high optical quality with a single emission peak centered at 394 nm that may be due to electron transitions from shallow defect levels of Cu^{2+} in the ZnO band-gap (see below). No visible emission due to deep defects was found for the investigated samples.

Figure 3a's inset shows the LED device structure based on the ZnO:Cu NW/p-GaN heterojunction used in the following experiments. More details on the experimental procedure can be found in our previous report.[4] Figure 3a shows a plot of *I–V* characteristics of the ZnO:Cu NW-based LED structure

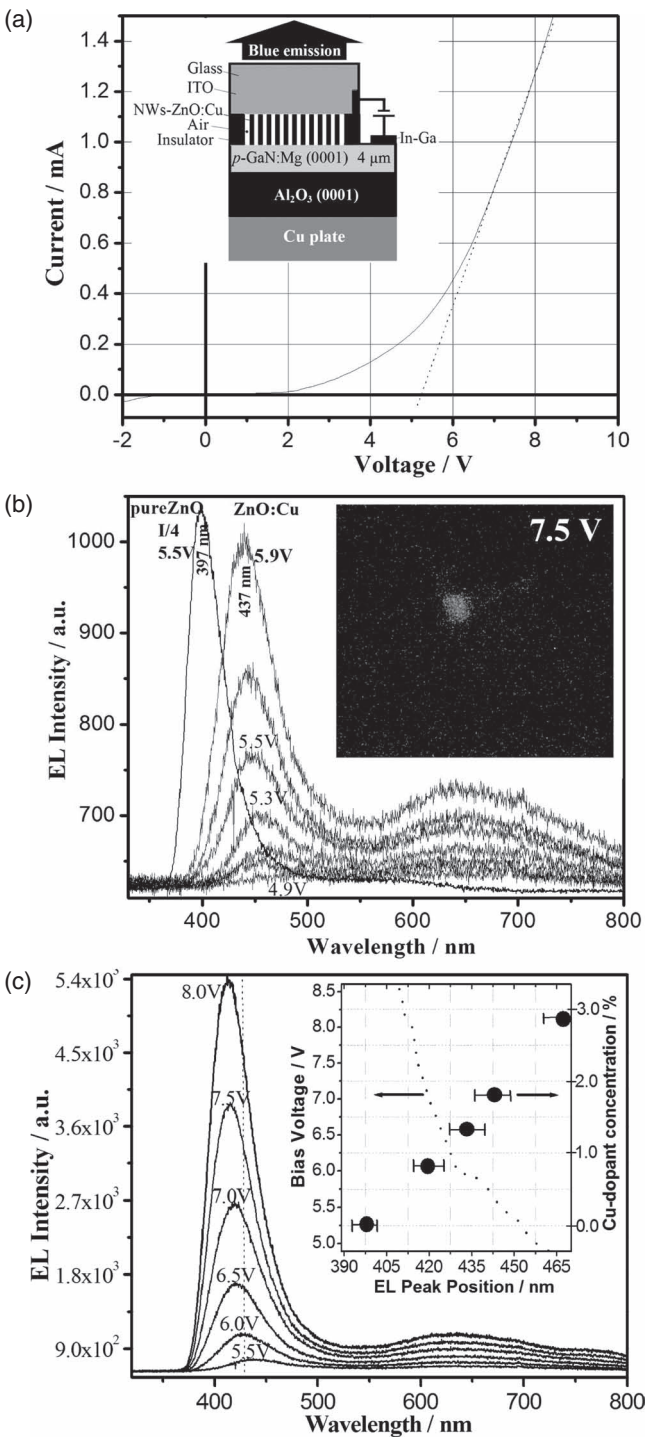

Figure 3. a) Current–voltage characteristic curve of an ITO/ZnO:Cu-NWs/p-GaN/In-Ga (ITO = indium tin oxide) heterojunction LED structure. Inset: Schematic configuration of the heterojunction LED structure; b) room-temperature electroluminescence spectra of the ITO/ZnO:Cu-NW/p-GaN/In-Ga heterojunction LED structure under different forward-bias low voltages (4.9–5.9 V). Inset: Image of the blue-light emission spot at room temperature under a dc bias of 7.5 V. c) is the same as (b), but for higher forward-biasing voltages (5.5–8.0 V). Inset: Shift of the main peak positions as a function of the forward-bias voltage and emission wavelength at 5.75 V versus Cu-dopant concentration in ZnO NWs.

© 2011 WILEY-VCH Verlag GmbH & Co. KGaA, Weinheim

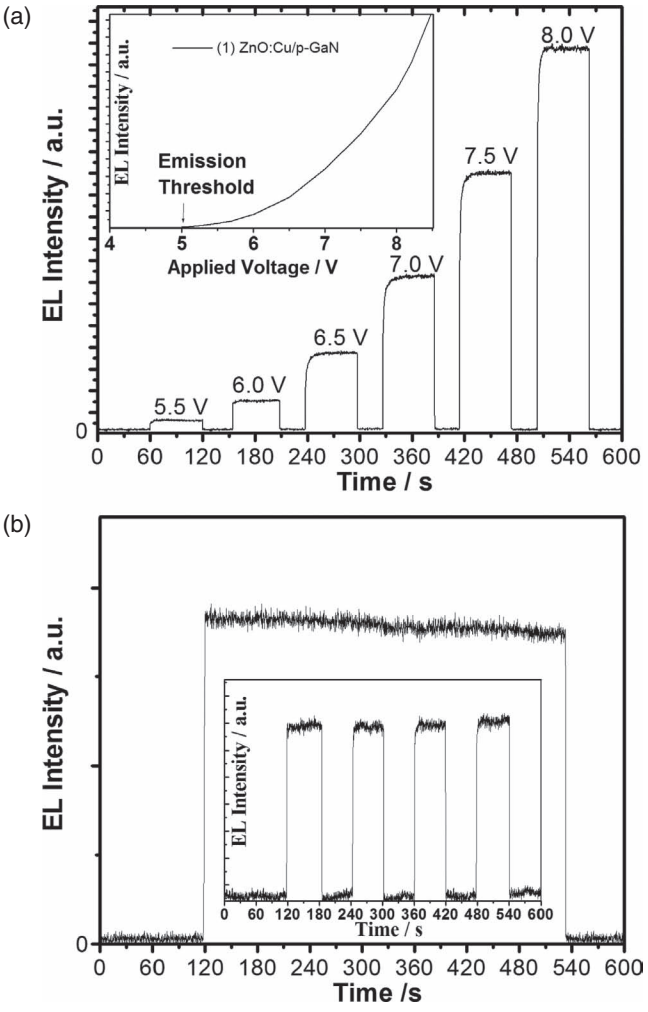

Figure 4. a) Time dependence of the RT-EL intensity and the forward-bias voltage of the fabricated ZnO:Cu NW-based LED structure with a step of +0.5 V. Inset: Relationship between the RT-EL intensity and the forward-bias voltage. b) Time dependence of RT-EL of the fabricated LED under dc bias of 6.5 V. Inset: RT-EL time dependence under dc bias of 6.5 V for four switch-on/switch-off pulses of 60 s.

measured in the dark at room temperature, with GaN as the positive pole. The device shows clear rectification character with a threshold voltage of about 2 V. Also, it can be seen that the reverse current of the heterojunction increases to –0.028 mA at about –2 V. In Figure 3b, the electroluminescence (EL) spectrum of the LED structure at different low forward-biased voltages is shown. The main EL emission peak shifted in wavelength by ca. 40 nm for the ZnO:Cu-based LED in comparison with that of the pure-ZnO-based device. The presence of a shifted EL peak position for ZnO:Cu/p-GaN with respect to that of pure ZnO/p-GaN structures provides evidence that holes are injected from p-GaN and recombine with electrons from the conductive n-ZnO:Cu NWs. This hypothesis is in agreement with previous observations on ZnO:Cu films in the literature.[21] In the inset of **Figure 4**a, it can be observed that the ZnO:Cu/p-GaN LED structure has an emission threshold voltage value of about 5 V, a value larger by about 0.6 V than in the pure-ZnO/GaN LED reported in our previous work.[3] This phenomenon may be attributed to a higher density of interfacial defects between ZnO:Cu and p-GaN thin films compared to the pure ZnO case. The electron and hole trapping in the region located near the ZnO:Cu nanowires and the p-GaN film, respectively, would result in an increased threshold and a reduced EL intensity as shown in Figure 3b.

At above 6.5–7.0 V, the emission could be seen with the naked eye. In the inset of Figure 3b the EL emission was imaged with a charge-coupled device (CCD) camera. A rounded spot was observed, which demonstrates that the emission arose from the whole disk-shaped (3 mm in diameter) active ZnO:Cu-NW layer electrodeposited on a square p-GaN substrate with larger area. As the biased voltage increased, the intensity of the main violet–blue peak rose exponentially (Figure 4a). In addition, by comparing Figure 3b and Figure 3c, we can note a much slower increase of the intensity of the visible emission due to deep defects compared to the increase of the violet–blue emission. Higher applied biases are favorable to the dominant violet–blue emission. Several phenomena can contribute to the EL emission peak, namely, band–band recombination, defect level band recombination and near-band-edge emission of ZnO and of GaN. Gruzintsev et al.[38] observed two visible emissions at about 2.27 and 2.55 eV in the PL spectra of Cu-doped ZnO films that corresponded to transitions from V_O to Cu_{Zn} levels of (Cu^+:$3d^{10}$) and (Cu^{2+}:$3d^9$), respectively. A green emission is classically reported for copper-doped ZnO.[18,39] However, in our experimental observations, no EL emission in the 2.27 eV region was found, but a broad band centered at 640 nm (see Figure 3b). This band could be due to oxygen interstitials, zinc vacancies,[40] or oxygen vacancies (V_O).[41] According to Peng et al.,[42] oxygen vacancies (V_O) give an energy level at –1.3 eV below E_c which can participate in EL emission and contribute significantly to the broad emission band centered at 640 nm (ca. 1.94 eV). However, further studies are necessary to check the exact origin of peaks which contributed to visible EL emission from ZnO:Cu/p-GaN heterostructures.

Our results show a wavelength emission shift by about 0.2 eV at low voltage between the main peaks observed experimentally in the EL of the diodes and in the PL spectra. This shift is classically observed for ZnO/GaN LEDs and in our previous work,[3,4] a similar shift was found between PL and EL (ca. 0.12 eV) measured from pure ZnO/p-GaN structure in exactly the same experimental conditions. PL is measured from the top part of the ZnO nanowires and is determined by the energetic structure of the NW material. On the other hand, EL emission is generated by carrier recombination at the near interface between the two semiconductors and is influenced by the energy properties of the ZnO/GaN heterojunction, notably by the energy offset between the conduction and the valence bands of ZnO and GaN (Figure S1 in the Supporting Information). We should also mention that due to the current flow in the device, the temperature of the emitting material may vary between the two experiments.

The near-band-edge emission peak wavelength depends on the applied forward bias. The inset in Figure 3c shows the dependency of the blue shift versus the applied bias. The behavior of the ZnO:Cu/GaN diode is different to that of similar pure ZnO-NW/GaN, for which the emitted wavelength was

© 2011 WILEY-VCH Verlag GmbH & Co. KGaA, Weinheim

stable with the applied bias.[3] The shift of the EL emission peak of ZnO/GaN LEDs has been reported in the literature and its physical origin is still under debate.[42–44] Under the driving force of an applied electric potential, the holes in the valence band of p-GaN move towards the ZnO NWs, and the electrons in the conduction band of the ZnO NWs move towards the GaN. The shape of the emission and its broadness compared to the PL spectrum suggest that EL is the contribution of several emission bands corresponding to several electronic processes (Figure S1). At the interface, the recombination of an electron in the conduction band and a hole in the valence band will produce a photon with relatively low energy. In the investigated structures, it seems likely that the two main contributions are, first, the radiative recombination at the interface ($h\nu_{inter}$ in Figure S1), for which the emission energy is reduced due to the energy offset of the valence and conduction bands between the two materials forming the heterojunction. The second contribution is the recombination in ZnO:Cu ($h\nu_{Cu}$ in Figure S1). By increasing the applied bias, the intensity of the latter contribution rises more rapidly than the former one, which causes a wavelength shift. The rather high wavelength of the emission suggests that the recombination in GaN is negligible because, for the GaN substrate, we noted no blue PL emission due to a transition between the conduction band and deep-Mg dopant levels. On the contrary, the contribution of bulk ZnO:Cu is strong, especially at rather high bias. It is probable that the shift is strongly influenced by the defects and the energy properties of the interface.

In the inset of Figure 3c, we showed the maximum emission wavelength measured at 5.75 V versus the Cu-dopant content in ZnO nanowires. This parameter was measured by EDX and was varied by changing the $CuCl_2$ concentration in the deposition bath. Since the data were obtained from several LED devices for every sample, the statistical error bars are shown in the figure. The EL emission wavelength increased gradually with the increase in Cu content, which suggests a continuous band-gap reduction with this parameter. We have also confirmed a gradual EL intensity decrease with increasing Cu content in ZnO since Cu introduces defects, notably near the interface, which act as nonradiative recombination centers.

Figure 4b illustrates that the violet–blue emission was relatively stable in intensity at the maximum of the LED emission peak. The intensity slightly decreased over 420 s by about 5%. We previously reported that the emission was stable in the case of pure ZnO emitters.[3] The emission slight variation may be due to heating with the increasing of the junction temperature, since the device structures were not encapsulated and not optimized with a special heatsink slug. The inset in Figure 4b shows that the maximum emission was reached quickly, less than 7 ms after device switch-on, and that the EL was immediately cut after the device switch-off. Switch-on/switch-off cycles at a forward bias of 6.5 V were studied on the ZnO:Cu-based LED structure without any observed degradation of the performance. This observation was confirmed with kinetic experiments presented in Figure 4a, which indicates the fast time response and system stability at different forward-bias voltages with an increment of +0.5 V between each next pulse.

To support and understand the above-reported experimental observations showing that the EL peak is shifted by about 0.28 eV from 397 to 437 nm after ZnO doping, we performed a computational analysis of the system. The theoretical energy-band diagram for pure ZnO and ZnO:Cu (doped at 0.8, 1.8, and 6.2 at.%) was drawn. Qualitatively, the same results were obtained for the three investigated concentrations and consequently only results obtained for the 1.8 at.% Cu concentration (close to the experimental concentration for 6 μM $CuCl_2$) are discussed. The quantitative influence of Cu concentration will be presented at the end of this section and in Table 1.

The electronic band structures of the pure ZnO and the Cu-doped ZnO systems are depicted in **Figure 5**a–c. The copper atom has an even number of electrons and consequently α and β spins are split. In our calculations an α-spin electron excess was chosen. Our results show that the Cu-doped ZnO system is a semiconductor for both α and β spins. The wide gap still remains when copper atoms are substituted for zinc atoms in the lattice. Previous theoretical studies by Xiong et al.[45] and Ye et al.[46] showed that this system is half-metallic (semiconductor for α spins and metallic for β spins). However, in these previous studies,[45,46] the gradient-corrected (GGA) functional PBE[47] was used and it is well-known that this family of functionals overestimates the electronic delocalization and gives rise to an appearance of metallic behavior for Cu-doped ZnO. In the present work, the use of a hybrid functional (PBE0, including 25% Hartree–Fock exchange) improves the description of electron localization, giving a more accurate and reliable description of the electronic structure of the system. As a consequence, a full semiconductor behavior of the Cu-doped ZnO system was found to be in good agreement with experimental results. From a qualitative point of view, the good electron localization on the Cu site is well-summarized by the computed spin-density maps depicted in Figures 1d,e. The excess α spin is essentially centered on the copper atom with a smaller contribution due to the delocalization on the surrounding oxygen atoms. The semiconducting behavior obtained when using the PBE0 functional is indeed fully consistent with the experimental rectifying characteristic of the Cu-doped ZnO/p-GaN heterojunction (Figure 3a).

For α spins (Figure 5b, Table 1, and Supporting information), the ZnO electronic structure was almost unaffected by the presence of Cu atoms. By analyzing the orbital contributions in the band structure, we observed that the valence-band edge is made of oxygen 2p and Zn 3d orbitals while the conduction-band edge is made of Zn 4s orbitals. These orbital contributions are identical to pure ZnO (Figure 5a). In the case of β spins (Figure 5c), the valence-band edge is a combination of Cu 3d and O 2p orbitals while the conduction-band edge is centered on the Cu atom (3d orbitals). We note that these two bands lie 0.35 eV above the ZnO valence-band edge and 0.12 eV below the ZnO conduction-band edge, respectively. This result is in agreement with experimental determination of defect levels in Cu-doped ZnO.[18,19] The DFT calculations exhibit a significant gap reduction for the β spins (3.65 eV) compared to in the pure ZnO system (3.93 eV; DFT calculations overestimate the absolute value of the band-gap). This gap reduction in the presence of copper dopant is in qualitative good agreement with experimental PL measurements where the gap is reduced by about 0.10 eV (between 382 and 394 nm). The phenomenon is also observed in EL spectra of the heterojunction between ZnO and

© 2011 WILEY-VCH Verlag GmbH & Co. KGaA, Weinheim

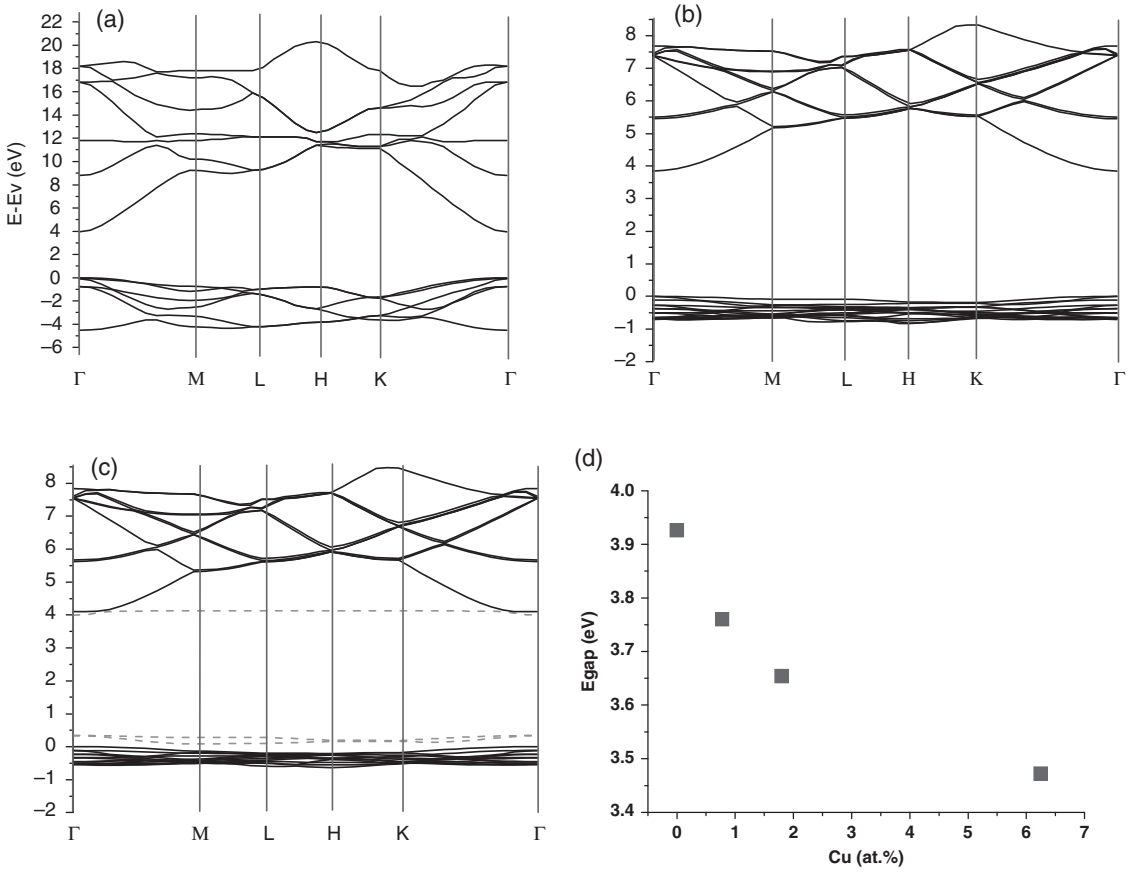

Figure 5. a) Computed band structures of pure ZnO, b) α spins, and c) β spins of Cu-doped ZnO (1.8 at.% Cu). In the case of β spins, the two dashed bands are centered on the copper atom, and are responsible for the band-gap reduction. d) Computed band-gap for β spins as a function of Cu atomic content in ZnO.

GaN systems, with a reduction of the emitted light energy by about 0.31 eV at low voltage (from 397 to 437 nm) between pure ZnO nanowires and Cu-doped ZnO nanowires.

Qualitatively, the effect has been confirmed by investigating theoretically two other concentrations: 0.8 at.% and 6.2 at.% (Table 1). The band-gap for β spins decreases with the copper-atom concentration in the hexagonal lattice because of the presence of bands centered on copper inserted inside the ZnO band-gap and because the broadness of the new bands increases with copper molar concentration. The computed density of states for each system is reported in the Supporting Information. The band-gap dependency on Cu concentration is reported in Figure 5d and Table 1. For 6.2 at.% of copper concentration, the gap is computed to be 3.47 eV which is 0.46 eV lower than the gap computed for pure ZnO (3.93 eV). To summarize, the DFT study clearly shows that the observed wavelength increase of EL light is due to the insertion of Cu 3d orbital states inside the ZnO gap (near-valence and conduction-band edges), which reduces the band-gap.

3. Conclusions

We have demonstrated a new low-temperature, efficient procedure for achieving copper-doping in ZnO nanowires that permits fine tuning of the band-gap energy of the nanostructures. The procedure was used to construct the first ZnO:Cu NW/p-GaN epitaxial heterojunction-based LED structure. We obtained a violet–blue EL emission for ZnO:Cu NW/p-GaN LED, shifted by about 40 nm at low voltage compared to emission of pure ZnO NW-based LEDs. A computational approach has been reported to support discussions on experimental data and has confirmed the possibility to tune the band-gap of ZnO NWs by Cu doping. The present results demonstrate that electrochemical techniques can be applied for band-gap engineering of ZnO NWs and adjustment of their emission wavelength. The present work is an important step forward in the fabrication of color-tunable light-emitting nanodevices. This developed method is novel, cost-effective, well-controlled, low-temperature, and occurs in nonaggressive environments; it can be used for any types of doping in NWs and is of great importance for further investigations/applications, notably related to LEDs.

4. Experimental Section

The substrates were magnesium-doped GaN(0001) layers grown on sapphire with the *c* axis perpendicular to the substrate (purchased from TDI, Inc corporation). The GaN layers were 3 µm thick with a dopant concentration of 3×10^{18} cm^{-3}. Prior to deposition, the p-GaN(0001)

© 2011 WILEY-VCH Verlag GmbH & Co. KGaA, Weinheim

substrate was degreased in trichloroethylene at 50 °C for 10 min, subsequently cleaned for 5 min in warm acetone at 53 °C in an ultrasonic bath, 10 min in methanol at room temperature in an ultrasonic bath, and rinsed with water. Then the substrate was etched for 10 min in concentrated ammonia (28%) at 60 °C, and finally rinsed with high-purity Millipore water. Cu-doped ZnO nanowires were synthesized at 90 °C using a potentiostatic procedure in a three-electrode electrochemical cell and a solution containing 0.2 mM $ZnCl_2$, $CuCl_2$ (99.99% $CuCl_2$, Aldrich), and 0.1 M KCl as supporting electrolyte and continuously bubbled with molecular oxygen.[3,4] The $CuCl_2$ concentration was varied between 0 and 15 μM. Electrodeposition was carried out at –1.2 V/SCE for 5000 s and controlled by an Autolab PGSTAT30 potentiostat/galvanostat and with a static working electrode (WE). Details on ECD of ZnO nanowires on p-GaN and fundamental physicochemical properties of cathodic ZnO nanowire synthesis in an aqueous zinc chloride solution of [$ZnCl_2$] = 0.2 mM have been reported previously.[3,4,37,48,49] The samples were then thermally annealed in air at 250 °C for 10 h before being included in the LED device structure. In this report we focus on two sets of samples: #1–pure ZnO NWs (for comparison purposes) and #2–Cu-doped ZnO NWs grown from a bath containing 6 μM $CuCl_2$ in electrolyte (about 1.2 at.% Cu/(Cu + Zn) in the nanomaterial determined by EDX titration). Two other Cu-dopant concentrations were also investigated. Starting from $CuCl_2$ concentration in the deposition bath at 3 and 15 μM gave rise to a Cu content in ZnO determined by EDX of about 0.8 at.% and 3 at.%, respectively. In the inset of Figure 3 only the most relevant results are presented, namely the EL main emission peak position which gradually shift with increasing Cu content in ZnO.

SEM images were obtained with an Ultra 55 Zeiss FEG at an acceleration voltage of 10 kV. Quantitative elemental analyses (EDX) were realized with a Bruker Li-drift silicon detector. For structural characterization, a high-resolution X-ray diffractometer Siemens D5000 operated with 40 kV and 45 mA using the CuKα radiation with λ = 1.5406 Å was employed. The XRD patterns were recorded in the 2θ range of 25°–130° with a scanning step of 0.02°. Room-temperature Raman scattering was measured with a Horiba Jobin-Yvon LabRam IR system in a back-scattering configuration. The 632.8 nm line of a He-Ne laser was used for off-resonance excitation with less than 4 mW power at the sample. Room-temperature PL was excited by the fourth harmonic (266 nm) of a YAG:Nd laser and dispersed with a HR250 monochromator (Jobin-Yvon) coupled to a UV-enhanced intensified charge-coupled device (ICCD; Roper). The electroluminescence measurements were collected by an optical fiber connected to a CCD Roper Scientific detector (cooled Pixis 100 camera) coupled with a SpectraPro 2150i monochromator. The monochromator focal lens was 150 mm, grating of 300 gr mm^{-1} blazed at 500 nm in order to record the emission of the ZnO in the whole near-UV-visible range.

LED devices were fabricated from the electrochemically prepared ZnO:Cu-NW/p-GaN epitaxial heterostructures as schematically illustrated in the inset of Figure 3a. The top of the ZnO wires was contacted with an ITO layer deposited on a transparent glass sheet. The top TCO (transparent conducting oxide) plate and the uncovered GaN layer were spaced using a thin insulator to avoid direct contact between the two layers. The GaN layer was contacted with In–Ga eutectic.

The Cu-doping of ZnO was theoretically characterized by periodic calculations which were carried out at the DFT level using the ab initio CRYSTAL09 code.[50] This code makes use of localized (Gaussian) basis sets and solves self-consistently Hartree–Fock and Kohn–Sham equations, thus allowing the efficient use of hybrid functionals for band-structure calculations. Calculations were performed at the DFT level by applying the hybrid-exchange-correlation functional PBE0.[51] Durand and Barthelat large core pseudopotential with (31/31) contractions were used on O atoms while large-core Hay and Wadt pseudopotentials with (111/111/41) contraction and the all-electron basis set (86 4111/6411/41) were considered for Zn and Cu atoms, respectively. This level of theory has already been proven to provide reliable geometrical and electronic properties of ZnO-based systems.[52] The wurtzite structure of ZnO was considered for all calculations. Cu doping was investigated by substituting one zinc atom with one copper atom in $(4 \times 4 \times 4)$, $(3 \times 3 \times 3)$, and $(2 \times 2 \times 2)$ supercells, which thus achieved a Cu concentration of 0.8 at.%, 1.8 at.%, and 6.2 at.%, respectively. The 1.8 at.% concentration is close to that obtained experimentally from a bath containing 6 μM $CuCl_2$. Comparisons were done between the Cu-doped ZnO and the bare ZnO system. Sampling of the irreductible Brillouin zone was done with 28 k-points for the primitive cell and 6 k-points for the supercells. During structural optimizations, all atomic positions and all cell parameters were allowed to freely relax. Because of the even number of electrons in copper, the density of states was split between α and β spins. The convention employed in this study is n_α–n_β = +1.

Supporting Information

Supporting Information is available from the Wiley Online Library or from the author.

Acknowledgements

The present work received the financial support of the C-nano Ile-de-France programme (granted NanoZnO-LED project). Dr. O. Lupan acknowledges the CNRS support as an invited scientist at the LECIME-ENSCP.

Received: January 31, 2011
Revised: May 4, 2011
Published online: July 29, 2011

[1] H. E. Brown, *J. Phys. Chem. Solid.* **1960**, *15*, 86.
[2] K. W. Liu, M. Sakurai, A. Aono, *J. Appl. Phys.* **2010**, *108*, 043516.
[3] O. Lupan, T. Pauporté, B. Viana, *Adv. Mater.* **2010**, *22*, 3298.
[4] O. Lupan, T. Pauporté, B. Viana, I. M. Tiginyanu, V. V. Ursaki, R. Cortès, *ACS Appl. Mater. Interfaces* **2010**, *2*, 2083.
[5] X. Wang, Q. Li, Z. Liu, J. Zhang, Z. Liu, R. Wang, *Appl. Phys. Lett.* **2004**, *84*, 4941.
[6] P. Kung, M. Razeghi, *Opto-Electron. Rev.* **2000**, *8*, 201–239.
[7] D. J. Rogers, F. H. Teherani, A. Yasan, K. Minder, P. Kung, M. Razeghi, *Appl. Phys. Lett.* **2006**, *88*, 141918.
[8] J. Li, S. H. Wei, S. S. Li, J. B. Xia, *Phys. Rev. B* **2006**, *74*, 081201.
[9] M. Snure, A. Tiwari, *J. Appl. Phys.* **2008**, *104*, 073707.
[10] D. C. Reynolds, D. C. Look, B. Jogai, *Solid State Commun.* **1996**, *99*, 873.
[11] D. M. Bagnall, Y. F. Chen, Z. Zhu, T. Yao, S. Koyama, M. Y. Shen, T. Goto, *Appl. Phys. Lett.* **1997**, *70*, 2230.
[12] C. Teng, J. Muth, U. Ozgur, M. Bergmann, H. Everitt, A. Sharma, C. Jin, J. Narayan, *Appl. Phys. Lett.* **2000**, *76*, 979.
[13] Y. S. Chang, K. H. Chen, *J. Appl. Phys.* **2007**, *101*, 033502.
[14] P. Dahany, V. Fleurovy, P. Thurianz, R. Heitzz, A. Hoffmannz, I. Broserz, *J. Phys.: Condens. Matter* **1998**, *10*, 2007.
[15] X. B. Wang, C. Song, K. W. Geng, F. Zeng, F. Pan, *Appl. Surf. Sci.* **2007**, *253*, 6905.
[16] S. U. M. Khan, M. Al-Shahry, W. B. Ingler, *Science* **2002**, *297*, 2243.
[17] Y. Yan, M. M. Al-Jassim, S.-H. Wei, *Appl. Phys. Lett.* **2006**, *89*, 181912.
[18] Y. Kanai, *J. Appl. Phys.* **1991**, *30*, 703.
[19] C. X. Xu, X. W. Sun, X. H. Zhang, L. Ke, S. J. Chua, *Nanotechnology* **2004**, *15*, 856.
[20] J. B. Kim, D. Byun, S. Y. Ie, S. H. Park, W. K. Choi, J. W. Choi, B. Angadi, *Semicond. Sci. Technol.* **2008**, *23*, 095004.
[21] T. S. Herng, S. P. Lau, S. F. Yu, S. H. Tsang, K. S. Teng, J. S. Chen, *J. Appl. Phys.* **2008**, *104*, 103104.
[22] X. Nie, S. B. Zhang, S. H. Wei, *Phys. Rev. B* **2002**, *65*, 075111.

© 2011 WILEY-VCH Verlag GmbH & Co. KGaA, Weinheim

[23] T. L. Phan, R. Vincent, D. Cherns, N. X. Nghia, V. V. Ursaki, *Nanotechnology* **2008**, *19*, 475702.
[24] S. M. Zhou, X. H. Zhang, X. M. Meng, K. Zou, X. Fan, S. K. Wu, S. T. Lee, *Nanotechnology* **2004**, *15*, 1152.
[25] N. Kouklin, *Adv. Mater.* **2008**, *20*, 2190–2194.
[26] H. J. Xu, H. C. Zhu, X. D. Shan, Y. X. Liu, J. Y. Gao, X. Z. Zhang, J. M. Zhang, P. W. Wang, Y. M. Hou, D. P. Yu, *J. Phys.: Condens. Mater.* **2010**, *22*, 016002.
[27] C. Xu, K. Yang, L. Huang, H. Wang, *J. Chem. Phys.* **2009**, *130*, 124711.
[28] H. Zhu, J. Iqbal, H. Xu, D. Yu, *J. Chem. Phys.* **2009**, *129*, 124713.
[29] O. Lupan, T. Pauporté, B. Viana, *J. Phys. Chem. C* **2010**, *114*, 14781.
[30] R. D. Shannon, *Acta. Crystallogr. Sect. A* **1976**, *32*, 751.
[31] Q. Ma, D. B. Buchholz, R. P. H. Chang, *Phys. Rev. B* **2008**, *78*, 214429.
[32] L.-H. Ye, A. J. Freeman, B. Delley, *Phys. Rev. B* **2006**, *73*, 033203.
[33] T. S. Jeong, *J. Appl. Phys.* **2004**, *96*, 175.
[34] P. K. Sharma, R. K. Dutta, A. C. Pandey, *J. Magn. Magn. Matter.* **2009**, *321*, 4001.
[35] Z. Wang, H. Zhang, L. Zhang, J. Yang, S. Yan, C. Wang, *Nanotechnology* **2003**, *14*, 11.
[36] K. Samanta, P. Bhattacharya, R. S. Katiyar, W. Iwamoto, P. G. Pagliuso, C. Rettori, *Phys. Rev. B* **2006**, *73*, 245213.
[37] T. Pauporté, E. Jouanno, F. Pellé, B. Viana, P. Aschehoug, *J. Phys. Chem. C.* **2009**, *113*, 10422.
[38] A. N. Gruzintsev, V. T. Volkoiv, I. I. Khodos, T. V. Nikiforova, M. N. Koval'chuk, *Russ. Microelectron.* **2002**, *31*, 200.
[39] G. U. Ozgur, Y. I. Alivov, C. Liu, A. Teke, M. A. Reshchikov, S. Dogan, V. Avrutin, S. J. Cho, H. Morkoç, *J. Appl. Phys.* **2005**, *98*, 041301.
[40] Y. W. Heo, D. P. Norton, S. P. Pearton, *J. Appl. Phys.* **2005**, *98*, 073502.
[41] X. Peng, J. Xu, H. Zang, B. Wang, Z. Wang, *J. Lumin.* **2008**, *128*, 297.
[42] M. C. Jeong, B. Y. Oh, M. H. Ham, S. W. Lee, J. M. Myoung, *Small* **2007**, *3*, 568.
[43] X. M. Zhang, M. Y. Lu, Y. Zhang, L. J. Chen, Z. L. Wang, *Adv. Mater.* **2009**, *21*, 2767.
[44] S. Xu, C. Xu, Y. Liu, Y. Hu, R. Yang, Q. Yang, Q. Yang, J. H. Ryou, H. J. Kim, Z. Lochner, S. Choi, R. Dupuis, Z. L. Wang, *Adv. Mater.* **2010**, *22*, 4749.
[45] Z. H. Xiong, S. Q. Shi, Q. X. Wan, F. Y. Jiang, *Phys. Scr.* **2007**, *T129*, 358.
[46] L.-H. Ye, A. J. Freeman, B. Delley, *Phys. Rev. B* **2006**, *73*, 033203.
[47] J. P. Perdew, K. Burke, M. Ernzerhof, *Phys. Rev. Lett.* **1996**, *77*, 3865.
[48] T. Pauporté, D. Lincot, B. Viana, F. Pellé, *Appl. Phys. Lett.* **2006**, *89*, 233112.
[49] H. Elbelghiti, T. Pauporté, D. Lincot, *Phys. Status Solidi A* **2008**, *205*, 2360.
[50] V. R. Saunders, R. Dovesi, C. Roetti, R. Orlando, C. M. Zicovich-Wilson, N. M. Harrison, K. Doll, B. Civalleri, I. Bush, Ph. D'Arco, M. Llunell, *Crystal 09 User's Manual*; Universita di Torino: Torino, Italy, **2009**.
[51] C. Adamo, V. Barone, *J. Chem. Phys.* **1999**, *110*, 6158.
[52] F. Labat, I. Ciofini, C. Adamo, *J. Chem. Phys.* **2009**, *131*, 044708.

© 2011 WILEY-VCH Verlag GmbH & Co. KGaA, Weinheim